Research Paper   Open Access

Study The Wear Properties of Al-Cr-Mo Grey Cast Iron Alloys Produced For Metal Cutting Tools Application

[1]Oyetunji, A., [2]Opaluwa, A. I. and [1]Seidu, S. O.
[1] Department of Metallurgical and Materials Engineering, Federal University of Technology, Akure, Ondo State Nigeria
[2] Department of Foundry Engineering, Federal Polytechnic, Idah, Kogi State. Nigeria
Corresponding Author: Oyetunji, A (akinlabioyetunji@yahoo.com)

ABSTRACT: *This work investigated the microstructures and wear properties of produced Al-Cr-Mo grey cast iron alloys from grey cast iron scraps for metal cutting tools application. Six different alloys of grey cast iron with major compositions of Fe-3%Al-2.5%Cr-2%Mo, Fe-3%Al-2%Cr-2%Mo, Fe-3%Al-2.5%Cr-1.5%Mo, Fe-3%Al-2%Cr-1.5%Mo, Fe-3%Al-1.5%Cr-1.5%Mo and Fe-3%Al-1.5%Cr-2%Mo were produced. The produced alloys were aged at ageing different temperatures of 150^oC, 200^oC, 250^oC, 300^oC and 350^oC for forty-eight hours. Their microstructural analysis after ageing was done using Scanning Electron Microscope (SEM) and Energy Dispersive Spectrometer (EDS). Also chemical analysis and wear analysis were conducted. The results of the chemical analysis showed the reduction in carbon, silicon and phosphorus contents thereby reduced carbon equivalent and changed the alloys from hypereutectic to hypoeutectic. The result of microstructural analysis shows that various microstructural phases such as nitrides, primary carbides and eutectic carbides were precipitated in the pearlitic matrix with eutectic carbide (Cr_7C_3) having the highest peak intensity in the XRD diffraction pattern. The wear rate decreases with the ageing temperature until 300^oC at which the minimum wear rate was obtained for each of the alloys, while wear resistance increases with the ageing temperature until 300^oC at which the maximum wear resistance was obtained for each of the alloys.*

Keywords: *Wear resistance; Abrasive; Microstructure; X-Ray Diffractometer (XRD); SEM Analysis*

I.   INTRODUCTION

Wear means a phenomenon in which materials are gradually exfoliated starting from the uppermost layers by mechanical action such as friction or abrasion [1]. Wear is a consequential removal of material from one or both of the surfaces in relative motion against each other [2]. Several factors, such as mechanical, thermal and chemical (corrosion) are associated with the process of wear. However, in most of the industrial applications involving material handling, abrasive wear plays a dominant role. Abrasion is a wear by displacement of material from surfaces in relative motion, caused by the presence of hard protuberances or by the presence of hard particles, either between the surfaces or embedded in one of them [2]. Abrasive wear may occur in dry state or in the presence of a liquid [2]. Wear mechanisms of abrasion, work material adhesion, attrition, tool fatigue, binder diffusion, coating delamination, and tribochemical wear can all contribute to tool wear. Abrasion predominately results in flank wear because of the movement across the tool of hard particles in the work material. High pressure applied by the machining on these particles can carry away small portions of the tool with the chips. The temperature and pressure on the tool flank and face during machining are large enough that permit atomic diffusion between the work material and tool [3]. The various wear testing methods are Sand-Falling Wear Resistance, Jet Wear Resistance, Reciprocating Motion Wear Resistance and Flat Disk Revolution Wear Resistance Test.In the context of machining, a cutting tool is any tool that is used to remove material from the work piece by means of shear deformation [4]. Cutting may be accomplished by single-point or multipoint tools. Single-point tools are used in turning, shaping, plaining and similar operations, and remove material by means of one cutting edge. Milling and drilling tools are often multipoint tools. Grinding tools are also multipoint tools. Each grain of abrasive functions as a microscopic single-point cutting edge and shears a tiny chip [4]. Some of these cutting tools commercially available are carbon tool steel, high speed steel (HSS) and cemented carbide [5]. Others are cast cobalt alloys, ceramics, cermet, cubic boron nitride (CBN) and

diamond. These are the most widely used cutting tools for taps, drills, reamers, gear tools, end cutters, slitting and broaches [4]. To produce quality product, a cutting tool must have four characteristics such as hardness to withstand abrasive force, ultimate tensile strength (UTS) to impact high stability (tools do not chip or fracture easily) even at high temperature, toughness to be able to absorb high energy and wear resistance in order for the tool to have acceptable tool life before calling for replacement [6].

Life of the tools used for machining plays a dominant role in machining cost. The standard practice for determining the life of the tools is to measure the progression of tool wear under specified conditions. Tool life is typically defined as the time to reach a pre-determined value of tool wear. The costs associated with tool wear and its importance to industry necessitates an understanding of tool wear and causes [3]. Therefore, this work is aimed at studying the wear properties of Al-Cr-Mo grey cast iron alloys produced for metal cutting tools.

1.1 Experimental Procedure

Solid solution and precipitation (ageing) techniques of strengthening materials were the methods used for this work. The wear properties determined are wear rate and wear resistance. Alloy materials include grey cast iron scraps; aluminium ingot of 2024 series according to ASTM unified numbering system (UNS), ferro-chromium of 67% purity, ferro-molybdenum of 55% purity and nitrided ferro-manganese of 75% purity to enrich the nitrogen content of the alloy.

1.2 Melting and Casting

Indirect electric arc furnace of 2 Kg capacity was used for the melting. The required quantity of the charging materials were weighed and charged into the furnace. Grey cast iron scraps were first charged and heated to the temperature of $1140^{o}C$ before the addition of alloy elements. Carbon (II) tetrachloride powder was added as a degasser. Nitrided ferro-manganese (Fe-75%MnN) was added to enrich the nitrogen content of the melt as well as to neutralize the harmful effect of the sulphur. Pouring was done at $1350^{o}C$ into a sand mould and was allowed to cool at room temperature for 12 hours before the casting was brought out of the mould.

1.3 Ageing Treatment

During ageing, samples were heated to $900^{o}C$, soaked for 30 minutes and transferred into salt-bath held at these different ageing temperatures of $150^{o}C$, $200^{o}C$, $250^{o}C$, $300^{o}C$ and $350^{o}C$ for forty-eight hours in each case [7, 8].

1.4 Chemical Analysis

Spetro-CJRO Arc-Spectrometer was used for chemical analysis of the developed grey cast iron alloys. Test piece whose surface was ground to ensure flatness was mounted on the sparking point of the spectrometer and the button pressed. After 30 – 40 seconds compositions were displayed on the monitor screen [9].

1.5 Microstructural Analysis

The microstructures of the produced alloys were analyzed using scanning electron microscope (SEM) model JEOL-2000FX, equipped with X-ray energy diffraction (XRD) and energy dispersive spectroscopy (EDS). Phase identification or microstructural morphology was carried out by SEM while the phase constituents and composition were quantified by XRD and EDS respectively [9].

1.6 Wear Analysis

Wear analysis was carried out using Taber's method. This was done by attaching sample to a rotating disc of 25 cm radius and pressure of a specified load was applied according to [10]. The samples used were 12 mm diameter by 40 mm long. The grit used was 220 rough with a revolution of 150 rpm. Exposing time for each sample on the wear test machine was 5 minutes and the density of cast iron used is 7.15 g/cm^3 respectively. After running through a fixed distance, the samples were removed, the weight loss due to wear was measured with digital weighing balance. Also wear rate and wear resistance were obtained in line with the work of [5].

2   RESULTS AND DISCUSSION

2.1 Chemical Analysis

Table 1 shows the chemical composition of the base metal (grey cast iron) and alloying elements used for this work. From Table 1, it was observed that the grey cast iron contains majorly 3.60% C, 2.50% Si, 0.90% Mn, 0.20% P and 0.1% S with carbon equivalent of 4.43. It is hypereutectic because, cast iron having carbon equivalent below 4.3% is hypoeutectic while above 4.3% is hypereutectic [11]. It belongs to class 30 grey cast iron based on its basic composition [12]. Ferro-chromium and ferro-molybdenum contains 67%Cr and 55%Mo as their purity while aluminium contains 96.93%Al as purity. According to ASTM unified numbering system (UNS), this aluminium belongs to 2024 series.

Table 1: Chemical Composition of the Base Materials used for the Work

Materials	Chemical Composition (%)												
	Fe	C	Si	Mn	P	S	Cr	Mo	Al	N	Cu	Ti	Mg
GCI	92.89	3.60	2.30	0.90	0.20	0.10	0.004	0.002	0.001	0.002	0.003	0.001	-
Fe-Cr	30.43	4.50	2.50	0.01	0.03	0.03	67.00	0.002	0.001	0.001	-	0.001	-
Fe-Mo	42.09	0.15	2.50	0.02	0.10	0.15	0.001	55.00	0.001	0.001	-	0.001	
Fe-MnN	15.78	0.15	1.00	75.0	0.05	0.02	-	-	0.002	8.00	-	0.001	-
Al	-	-	0.001	0.02	-	-	-	-	96.93	0.001	3.00	0.001	0.04

Table 2 shows chemical composition of the developed grey cast iron alloys. On the addition of alloying elements there was slight reduction in carbon, silicon and phosphorus contents. Carbon was reduced from 3.60% to 3.43%. Silicon was reduced from 2.50% to 2.30% and phosphorus from 0.20 to 0.15%. With this composition, the carbon equivalent has been reduced from 4.43 to 4.25. The alloys have become hypoeutectic. This is line with the previous work [9], that as-cast microstructure changed from hypereutectic to hypoeutectic with the increase of alloying element. It was also noticed that the nitrogen content was increased to 0.500%.

Table 2: Chemical Composition of the Developed Grey Cast Alloys

Alloys No	Chemical Composition (%)											
	C	Si	Mn	P	S	Mg	Mo	Al	N	Ti	Cr	Fe
Alloy 1	3.43	2.31	1.041	0.15	0.102	0.02	1.500	3.000	0.50	0.004	2.010	Bal
Alloy 2	3.43	2.31	1.041	0.15	0.102	0.02	1.500	3.000	0.50	0.004	1.510	Bal
Alloy 3	3.43	2.31	1.041	0.15	0.102	0.02	2.000	2.990	0.50	0.004	1.510	Bal
Alloy 4	3.43	2.30	1.041	0.15	0.102	0.02	1.500	3.001	0.50	0.004	2.510	Bal
Alloy 5	3.43	2.30	1.041	0.15	0.102	0.02	2.000	3.000	0.50	0.004	2.501	Bal
Alloy 6	3.44	2.30	1.041	0.15	0.102	0.02	2.001	3.001	0.50	0.004	2.001	Bal

2.2 Microstructural Analysis

Plate 1 shows the micrograph of the base metal used for the work. The grain particles are mostly made up of graphite flakes in pearlitic matrix. Microstructures consist of dark graphite existing in the form of flakes, which reside inside pearlite matrix. It is the micrograph of the grey cast iron sample without deliberate additions of any alloying elements. The micro-structure represents a typical grey cast iron with large volume of soft graphite flakes embedded in the matrix of the microstructure.
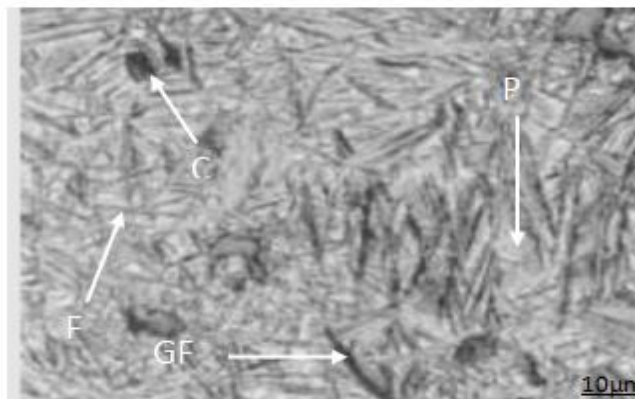

Plate 1: Micrograph of the Base Metal (Grey Cast Iron)
C = Cementite, P = Pearlite, GF = Graphite Flake, F = Ferrite.

Plate 2a shows the SEM micrograph of grey cast iron alloys 1. The phases present are Cr_7C_3, AlN, Mo_3C, $AlFe_2N$, FeCr, FeC, Fe_5C_2 and $AlFe_5C_2$. Plate 2b shows the SEM micrograph of grey cast iron alloys 2. The phases present are Cr_7C_3, AlN, Mo_3C, $AlFe_2N$, Fe_5C_2 and $AlFe_5C_2$. Plate 2c shows the SEM micrograph of grey cast iron alloys 3. The phases present are Cr_7C_3, AlN, Mo_3C, FeCr, FeC, Fe_5C_2 and $AlFe_5C_2$. Plate 2d shows the SEM micrograph of grey cast iron alloys 4. The phases present are Cr_7C_3, AlN, Mo_3C, $AlFe_2N$, FeCr, FeC, Fe_5C_2 and $AlFe_5C_2$. Plate 2e shows the SEM micrographs of grey cast iron alloys 5. The phases present are Cr_7C_3, AlN, Mo_3C, $AlFe_2N$, FeCr, Fe_5C_2 and $AlFe_5C_2$. Plate 2f shows the SEM micrographs of grey cast iron alloys 6. The phases present are Cr_7C_3, AlN, Mo_3C, $AlFe_2N$, FeCr, FeC, Fe_5C_2 and $AlFe_5C_2$.
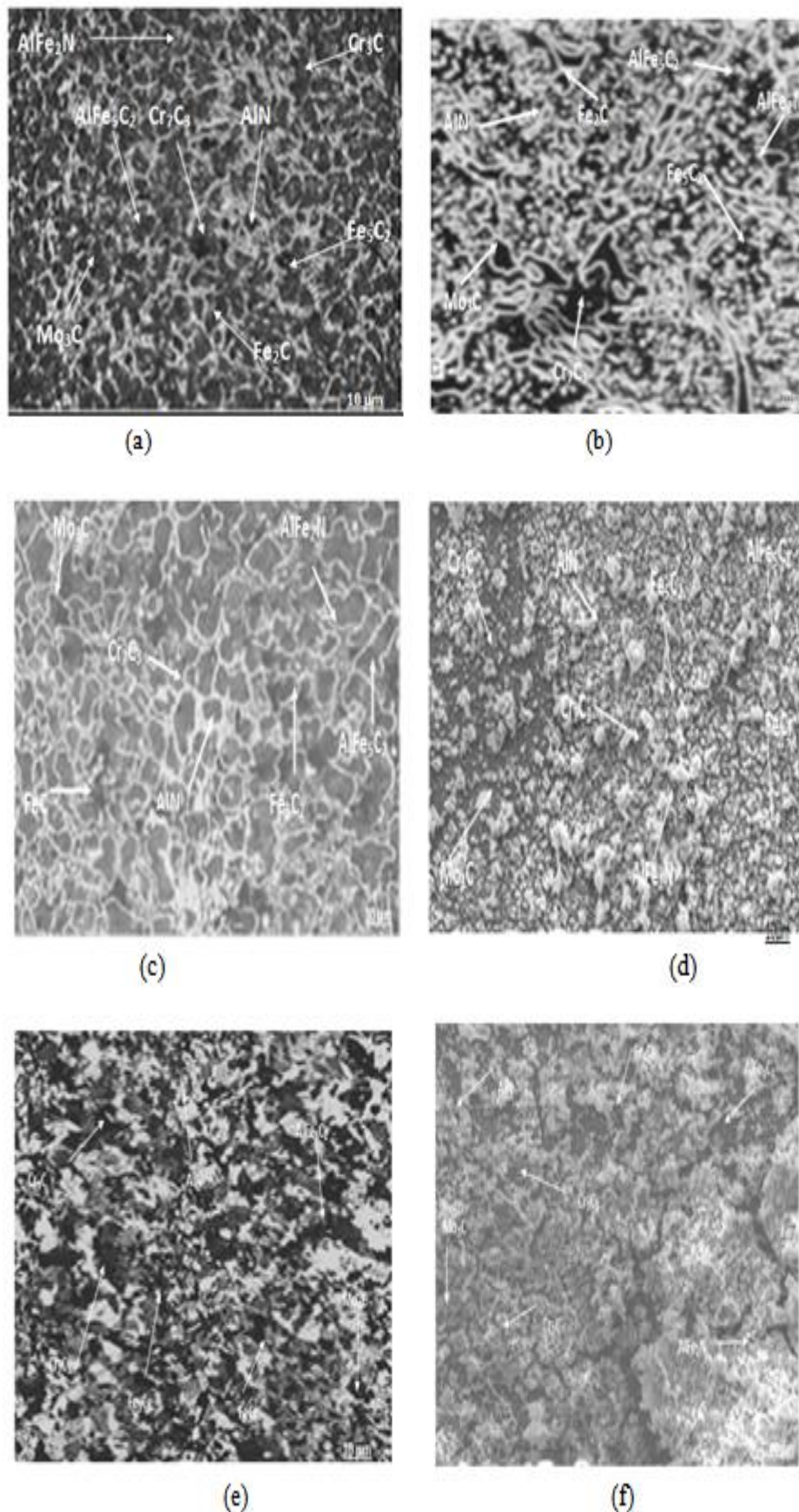
Plate 2: The SEM Micrographs of the developed Grey Cast Iron Alloys. (a), (b), (c), (d), (e) and (f) represent Alloys 1, 2, 3, 4, 5 and 6 respectively.

Plates 2a – f shows the spectra and intensities of the phases quantified by XRD. From the XRD diffraction pattern, aluminium nitride (AlN) has its peak intensity of 120 Counts S^{-1}, 100 Counts S^{-1}, 99.1 counts S^{-1}, 20.5 Counts S^{-1} and 20.5 Counts S^{-1} in Figures 1a, b, c, d, e and f at $2\theta = 39.854$ respectively. Among the carbides phases present, only Cr_7C_3 has the highest peak intensity in each of the alloys. Its peaks intensity are 660 Counts S^{-1}, 467 Counts S^{-1}, 466 Counts S^{-1}, 450 Counts S^{-1}, 121 Counts S^{-1}, 121 Counts S^{-1} in Figures 1a, b, c, d, e and f at $2\theta = 48.947$ respectively.
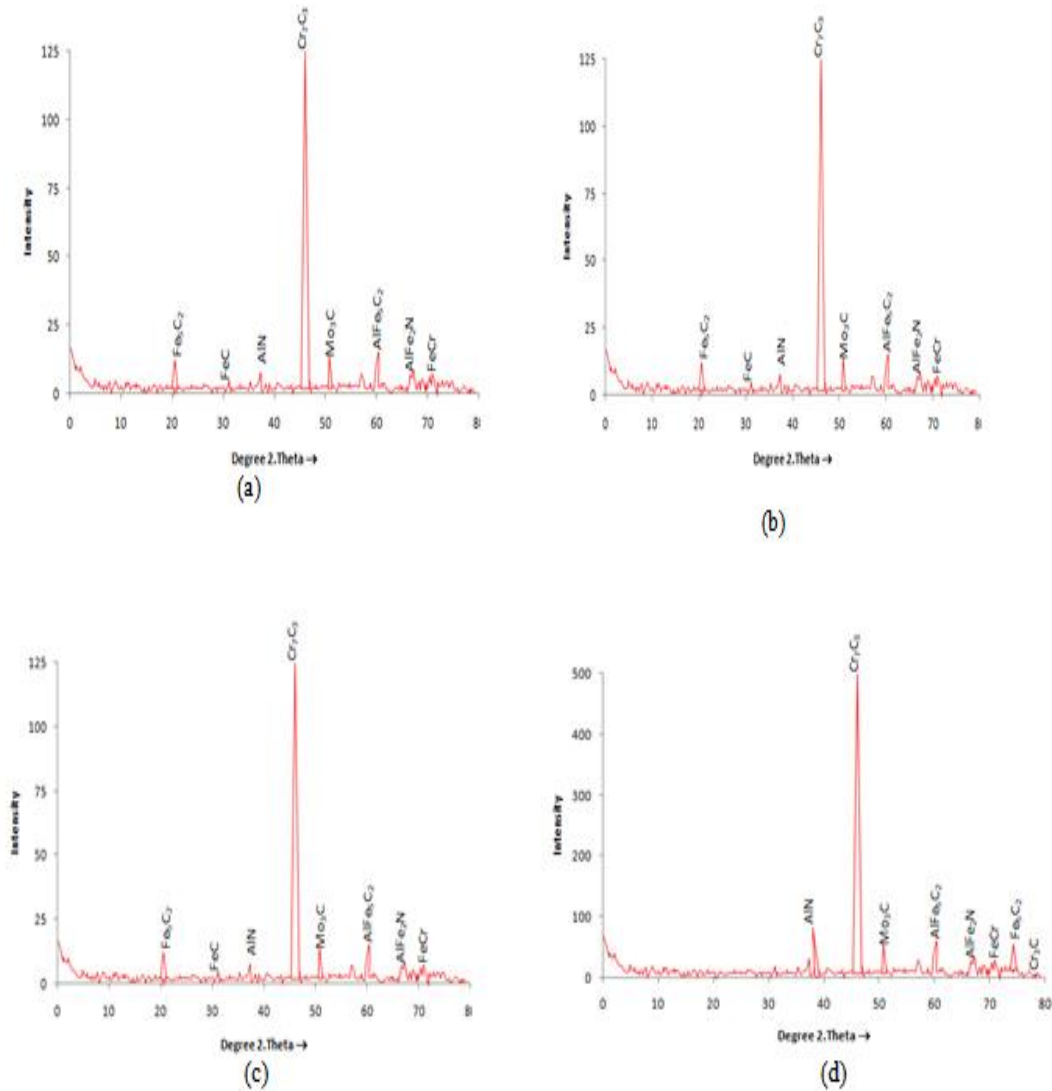
Figure 1: XRD Patterns of the Developed Grey Cast Iron Alloys Aged at 300°C for 48 hours. (a). (b), (c), (d), (e) and (f) represent Alloys 1, 2, 3, 4, 5 and 6 respectively.

The phase compositions quantified by EDS are shown in Tables 3 - 8. Interstitial solid solution of nitrogen and aluminium (AlN) was formed at 55.4%wtAl-12.5%wtN while that of carbon and chromium (Cr_7C_3) was at 66.2%wtCr-15.8%wtC. At this phase composition, Cr and C are within their maximum spinodal regions and this gave rise to high peak intensity of Cr_7C_3 (13).

Table 3: EDS Parameters of Alloy 1 Aged at 300°C for 48 hours

Phase Composition by EDS					
phase	C	Al	Cr	Mo	N	Fe
Fe_5C_2	25.5					74.5
FeC	24.7					75.3
AlN		55.4			12.5	32.1
Cr_7C_3	15.8		66.2			18.0
Mo_3C	20.1			50.2		29.7
$AlFe_5C_2$	22.5	48.9				28.6
$AlFe_2N$		43.4			15.6	41.0
FeCr			44.3			53.7

Table 4: XRD and EDS Parameters of Alloy 2 Aged at 300°C for 48 hours

Phase Composition by EDS					
phase	C	Al	Cr	Mo	N	Fe
Fe_5C_2	25.5					74.5
FeC	24.7					75.3
AlN		55.4			12.5	32.1
Cr_7C_3	15.8		66.2			18.0
Mo_3C	20.1			50.2		29.7
$AlFe_5C_2$	22.5	48.9				28.6
$AlFe_2N$		43.4			15.6	41.0
FeCr			44.3			53.7

Table 5: XRD and EDS Parameters of Alloy 3 Aged at 300°C for 48 hours

Phase Composition by EDS					
phase	C	Al	Cr	Mo	N	Fe
Fe_5C_2	25.5					74.5
FeC	24.7					75.3
AlN		55.4			12.5	32.1
Cr_7C_3	15.8		66.2			18.0
Mo_3C	20.1			50.2		29.7
$AlFe_5C_2$	22.5	48.9				28.6
$AlFe_2N$		43.4			15.6	41.0
FeCr			44.3			53.7

Table 6: XRD and EDS Parameters of Alloy 4 Aged at 300°C for 48 hours

Phase Composition by EDS					
phase	C	Al	Cr	Mo	N	Fe
Fe_5C_2	25.5					74.5
AlN		55.4			12.5	32.1
Fe_2C	23.7					76.3
Cr_7C_3	15.8		66.2			18.0
Mo_3C	20.1			50.2		29.7
$AlFe_5C_2$	22.5	48.9				28.6
$AlFe_2N$		43.4			15.6	41.0
FeCr			44.3			53.7

Table 7: XRD and EDS Parameters of Alloy 5 Aged at 300°C for 48 hours

Phase Composition by EDS					
Phase	C	Al	Cr	Mo	N	Fe
AlN		55.3			12.5	32.1
Cr_7C_3	15.8		66.2			18.0
Mo_3C	20.0			50.4		29.6
$AlFe_5C_2$	22.3	48.4				29.3
FeCr			44.5			53.5
Fe_5C_2	24.8					75.2
Cr_3C	19.6		54.3			26.1

**Table 8**: XRD and EDS Parameters of Alloy 6 Aged at 300°C for 48 hours

Phase Composition by EDS						
Phase	C	Al	Cr	Mo	N	Fe
AlN		55.3			12.5	32.1
Cr_7C_3	15.8		66.2			18.0
Mo_3C	20.0			50.4		29.6
$AlFe_5C_2$	22.3	48.4				29.3
$AlFe_2N$		44.0			15.5	40.5
FeCr			44.5			53.5
Fe_5C_2	24.8					75.2
Cr_3C	19.6		54.3			26.1

3.3 Wear Resistance

Figure 2 shows the variation of wear resistance with ageing temperature. The wear resistance increases with ageing temperature until 300°C before starting to decrease. The increase in the wear resistance is due to increase in hardness. The maximum wear resistance was obtained for all the alloys at the ageing temperature between 290°C and 310°C. This maximum wear resistance occurs at critical size and distribution of the intermetallic particles, some of which have coherent stress field around them. Above 310°C which is the peak ageing temperature, particles coarsing occurred and subsequently lead to the reduction in wear resistance.

The increase in the wear resistance depends upon the microstructures as in Plates 1 and 2. Pearlitic matrix gives high wear resistance than ferritic matrix (5). Pearlitic matrix instead of ferritic matrix was formed to accommodate phases such as nitrides and carbides (1) and (14). It is the presence of these phases in pearlitic matrix that led to increase in wear resistance (14). Nitrides and carbides of different phases such as primary carbide (MC_3), eutectic carbide (M_7C_3) and secondary carbide ($M_{23}C_6$) were formed.

During ageing, these phases are precipitated and evenly dispersed throughout the matrix to offer resistance to dislocation motion thereby improve the wear properties (12). There is increase in wear resistance due to multiple precipitates of different phases with different orientations (i.e. nitrides are precipitated interstitially while the carbides formed are precipitated substitutionally within the same matrix). It has been observed that those alloys with high wear resistance values have low wear rate (15).
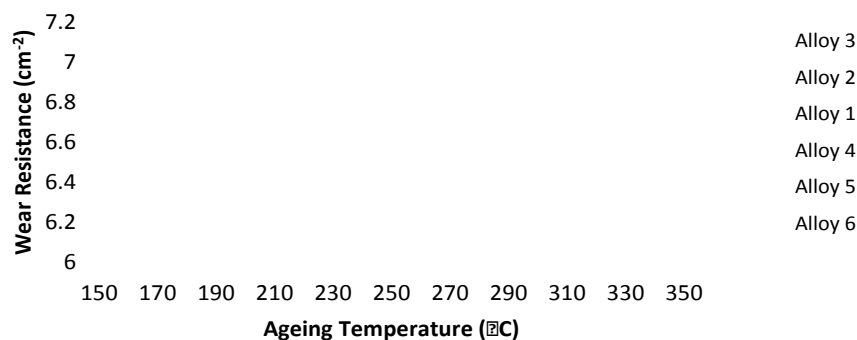
Fig. 2: Variation of Wear Resistance with Ageing Temperature of the Produced Alloys

3 CONCLUSIONS

The following conclusions were drawn from the study:
1. The increase in the wear resistance depends upon the microstructures.
2. Pearlitic matrix was formed that give high wear resistance than ferritic matrix.
3. Pearlitic matrix instead of ferritic matrix was formed to accommodate phases such as nitrides and carbides.
4. The presence of these phases (nitrides and carbides) in pearlitic matrix that led to increase in wear resistance. Nitrides and carbides of different phases such as primary carbide (MC_3), eutectic carbide (M_7C_3) and secondary carbide ($M_{23}C_6$) were formed.
5. There is increase in wear resistance due to multiple precipitates of different phases with different orientations (i.e. nitrides are precipitated interstitially while the carbides formed are precipitated substitutionally within the same matrix).
6. It has been observed that those alloys with high wear resistance values have low wear rate.

7. Fe-3%Al-2%Cr-2%Mo; Fe-3%Al-2.5%Cr-2%Mo; Fe-3%Al-2.5%Cr-1.5%Mo; Fe-3%Al-2%Cr-1.5%Mo; Fe-3%Al-1.5%Cr-1.5%Mo and Fe-3%Al-1.5%Cr-2%Mo have the maximum wear resistance of 7.15 cm^{-2} x 10^6, 6.88 cm^{-2} x 10^6, 6.7 cm^{-2} x 10^6, 6.65 cm^{-2} x 10^6, 6.5 cm^{-2} x 10^6 and 6.36 cm^{-2} x 10^6 respectively.

REFERENCES

[1]. Kennedy, D. M. and Hashmi, M. S. J. (1998); Method of Wear Testing for Advance Surface Coating and Bulk Materials. Journal of Materials Processing Technology. Vol. 77. Pp. 246 – 253.

[2]. Jawaharial, N. (2006); Measurement of Abrasive Wear Properties of Metallic Materials. Journal of Indian Standard Methods of Materials Measurement. ISB 10636 (Vol.1). pp. 1983 – 1986.

[3]. Harris, S. G, Doyle, E. D., Vlasveld, A. C., Audy, J. and Quick, D. (2003); A Study of the Wear Mechanisms of Ti-AlN and Ti-Al-CrN Coated High Speed Steel Twist Drills under dry Machining Condition. ELSEVIER.www.elservier.com/locate/wear. Pp. 723 – 734.

[4]. Stephenson, D. A. and Agapiou, J. S. (1997): Metal Cutting Theory and Practice, Marcel Dekker. Pp. 164, ISBN 978-0-8247-9579-5.

[5]. Marinov, V. (2007); Cutting Tool Requirements. Manufacturing Technology. Pearson Prentice Hall Ltd. USA Pp. 86 – 88.

[6]. Schneider, G. (2009); Cutting Tool Materials. American Machinist. Pp. 123

[7]. Callister, W. D. (2000); Fundamentals of Materials Science and Engineering. John Wiley & Sons, Inc. New York. Pp 69-185.

[8]. Opaluwa, I.; Oyetunji, A. and Seidu, S. O. (2015). Age Strengthening of Grey Cast Iron Alloys for Machine Cutting Tools Production. Journal of Minerals and Materials Characterization and Engineering, 3. Pp.107-117.

[9]. Youping, M. A., Xlulan, L. J., Yugoa, L. I. U. and Xlaoving, D. (2013); Microstructures and Properties of Ti-Nb-V-Mo Alloyed High Chromium Cast Iron. BULL Materials Science. Vol. 36 (5).Pp 839 – 844.

[10]. Friedrich, F.; Edwald, B. and Martin, K. (2009); Advanced Methods of Characterization of Abrasion Resistance of Wear Protection Materials. FME Transactions. Vol. 37. Pp. 61-70.

[11]. Khanna, O. P. (2009); Materials Science and Metallurgy. Dhanpat Rail Publication Limited, New Delhi. Pp. 17-1 to 17-12.

[12]. Anish, T. V. (2002); Age Strengthening of Gray Cast Iron: Alloying Effects and Kinetic Study. AFS Transactions, paper 02-120, Pp. 995-1002.

[13]. Yoshiro, S; Yoshiyuki, S; Kazumi, O; Takahiro, A; Kanako, G. and Kotaro, A. (2002); Kinetic of Phase Separation in Fe-Cr-Mo Ternary Alloys. Materials Transactions, Vol. 43 (2). Pp 271-276.

[14]. Agarwal, R. I; Banga, T. R. and Tahil, M. (2007); Foundry Engineering. Hanna Publishers; Delhi. Pp. 22-56.

[15]. Ogunsoye, J. O, Talabi, S. I., Olumuyiwa, I. A. and Afemefuna, T. (2013); Effect of Silicon Addition on the Wear Properties of Grey Cast Iron. Journal of Minerals and Materials Characterization and Engineering. Vol. 1.Pp 61 – 67.